

## Understanding ultrafast carrier dynamics in single quasi-one-dimensional Si nanowires

M. A. Seo,<sup>1,a)</sup> S. A. Dayeh,<sup>1</sup> P. C. Upadhyaya,<sup>1,2</sup> J. A. Martinez,<sup>3</sup> B. S. Swartzentruber,<sup>3</sup> S. T. Picraux,<sup>1</sup> A. J. Taylor,<sup>1</sup> and R. P. Prasankumar<sup>1,a)</sup>

<sup>1</sup>Center for Integrated Nanotechnologies, Los Alamos National Laboratory, Los Alamos, New Mexico 87545, USA

<sup>2</sup>Indian Institute of Science Education and Research, Kolkata 741252, India

<sup>3</sup>Center for Integrated Nanotechnologies, Sandia National Laboratories, Albuquerque, New Mexico 87185, USA

(Received 5 January 2012; accepted 26 January 2012; published online 15 February 2012)

We use femtosecond optical pump-probe spectroscopy to study ultrafast carrier dynamics in single quasi-one-dimensional silicon nanowires. By isolating individual nanowires, we avoid complications resulting from the broad size and alignment distribution in nanowire ensembles, allowing us to directly probe ultrafast carrier dynamics. Spatially-resolved experiments demonstrate the influence of surface-mediated mechanisms on carrier dynamics in a single NW, while polarization-resolved experiments reveal a clear anisotropy in carrier lifetimes measured parallel and perpendicular to the long axis of the NW, due to density-dependent Auger recombination. These results suggest the possibility of tailoring carrier relaxation in a single nanowire for a desired application. © 2012 American Institute of Physics. [doi:10.1063/1.3685487]

In recent years, much interest has been shown in the optical properties of silicon nanowires (SiNWs) for their wide range of potential applications, particularly in enabling nanoscale optoelectronic circuitry, transistors, and solar cells.<sup>1–3</sup> These quasi-one-dimensional (1D) nanosystems have unique properties that depend on their size, shape, and alignment, which are often studied by photoluminescence (PL) spectroscopy. While time-integrated and time-resolved PL experiments have given some insight into the influence of the NW diameter,<sup>4</sup> defect states,<sup>5</sup> and incident light polarization relative to the long axis of the NW,<sup>6,7</sup> these measurements have not had sufficient time resolution to resolve several important carrier relaxation processes, including electron-phonon coupling and inter/intravalley scattering. Therefore, there remains a lack of basic understanding on how light interacts with individual NWs on an ultrashort time scale. In contrast, femtosecond optical pump-probe spectroscopy does have sufficient time resolution (<100 femtoseconds (fs)) to resolve fundamental dynamical processes in NWs. However to date, nearly all ultrafast optical experiments on semiconductor NWs have been done on NW ensembles,<sup>8–15</sup> in which the broad distribution of NW sizes and orientations can introduce measurement artifacts, limiting the insight obtained from these studies.

These considerations have motivated the current interest in exploring carrier dynamics in individual NWs. However, due to the difficulty in isolating and finding an individual NW on a substrate, as well as the small signal levels inherent to ultrafast optical experiments on single NWs, there have only been a few studies of femtosecond carrier dynamics in single NWs,<sup>16,17</sup> and not yet in Si, arguably the most important NW material of all. From this viewpoint, it is especially worth investigating the size- and polarization-dependence of

carrier dynamics in individual NWs to understand their intrinsic properties without the influence of inhomogeneous broadening, which will then enable researchers to utilize their unique directional optical properties in different applications.<sup>18,19</sup> Since their surface to volume ratio varies directly with diameter, many properties of NWs are governed by their size, including carrier relaxation, surface recombination velocity, and diffusion length. The polarization of the incident light can also play an important role in NW properties and applications. For example, although the vast majority of solar cell modules are based on crystalline Si, there have been several attempts to make SiNW solar cells for enhanced charge transport.<sup>20,21</sup> Because these devices have p-n junctions in either the radial<sup>22</sup> or axial<sup>23,24</sup> directions, it is essential to understand the different physical processes that can influence the lifetimes of photoexcited carriers collected in a direction parallel or perpendicular to light absorption.<sup>25</sup> To date, ultrafast measurements on SiNW ensembles have not resolved the influence of the incident polarization on the carrier lifetime,<sup>11</sup> making single NW measurements essential.

We have measured ultrafast carrier dynamics in single SiNWs by using non-degenerate pump-probe spectroscopy to excite and probe carriers above the indirect band gap of Si ( $E_g = 1.12$  eV). In particular, we observe a strong position- and polarization-dependence of the transient carrier dynamics in single SiNWs, which then enables us to separately determine the influence of surface-mediated mechanisms and density-dependent Auger recombination on carrier relaxation, giving deep insight into light-matter interactions in these quasi-1D-systems. These results will have significant implications for SiNW-based applications ranging from high speed transistors to solar cells.

We used a non-degenerate femtosecond pump-probe system to measure polarization-dependent transient carrier dynamics in SiNWs. The output of a 30 femtosecond Ti:sapphire

<sup>a)</sup>Authors to whom correspondence should be addressed. Electronic addresses: minahseo@lanl.gov and rpprasan@lanl.gov.

laser oscillator, operating at 80 MHz at a center wavelength of 840 nm, is divided into pump and probe beams, with the probe power  $<10\%$  of the pump power. The pump beam is then frequency doubled in a BBO crystal to generate 420 nm pulses. The initial magnitude of the normalized photoinduced change in probe transmission,  $\Delta T/T$ , was  $\sim 10^{-5}$ . Using a 10X microscope objective lens, the back side of the sample is imaged onto a CCD camera to overlap the pump ( $\sim 25 \mu\text{m}$  diameter) and probe ( $\sim 20 \mu\text{m}$  diameter) at a certain position on a given SiNW. Placing broadband linear polarizers and wave plates in the path of both beams enables us to measure  $\Delta T/T$  signals as a function of the light polarization relative to the NW axis.

The SiNWs used for these experiments were grown through vapor-liquid-solid (VLS) synthesis, using cold wall chemical vapor deposition with 50% silane in hydrogen and catalytic Au growth seeds.<sup>26</sup> The NWs were dry transferred onto a sapphire substrate with an areal density of  $\sim 5.5 \times 10^6$  NWs/cm<sup>2</sup>, diameters of  $d = 50\text{--}240$  nm, and lengths of  $l \sim 80 \mu\text{m}$ . These well aligned NW arrays are used in our measurements on ensembles (Fig. 1(a)). Individual SiNWs were then picked up using a nanomanipulator developed at our center that consists of a field-emission SEM (JEOL 6701 F) modified to include 2 probe tips. These NWs were then placed onto a gold patterned sapphire substrate, which enables us to repeatedly find their positions. Two types of NWs, straight (Fig. 1(b)) and bent (Fig. 1(c)), are examined in our experiments.

Ultrafast optical pump-probe experiments were performed in reflection on bulk silicon and in transmission on SiNW ensembles and a single SiNW sample (Fig. 1(d)). In general, the photoinduced change in the probe reflection in bulk Si is sequentially induced by electron-hole pair excitation, intraband carrier energy relaxation, and trapping/recombination processes.<sup>9,11,27</sup> In contrast to bulk Si, curve fits to our data reveal that the  $\Delta T/T$  signal decays in several tens of picoseconds (ps) for the ensemble NW sample and the single NW sample. The faster relaxation in the NW ensemble as compared to bulk Si can be explained by the increased influence of surface traps and recombination cen-

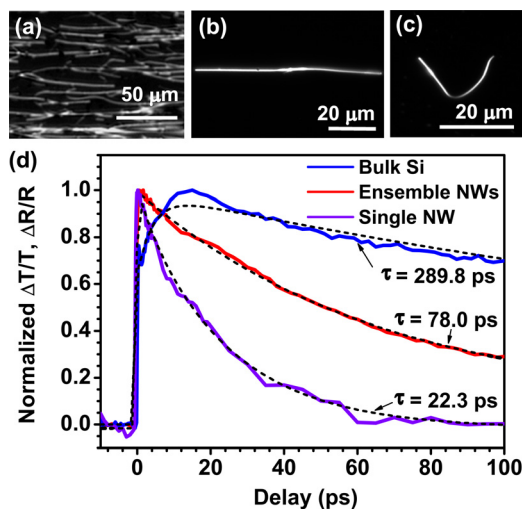


FIG. 1. (Color online) Dark field optical microscope images are shown for (a) 50-240 nm diameter ensemble SiNWs, (b) a straight single SiNW, and (c) a bent single SiNW. (d) Comparison of transient carrier dynamics between ensemble and single SiNWs and bulk silicon, measured for  $E_{||}$  and  $P_{||}$ .

ters as the degree of spatial confinement increases.<sup>11</sup> Carrier relaxation is even faster in the single NW, although this depends on the specific size and morphology of a given NW.

The single NW that we focus on in this work has a tapered shape, as determined through SEM measurements. Due to this tapered geometry, the measured photoinduced transmission change at different positions on the same NW directly reveals the diameter dependence of the carrier dynamics (Fig. 2(a)). The normalized  $\Delta T/T$  signals at four different positions ( $P_1$ ,  $P_2$ ,  $P_3$ , and  $P_4$ ) are shown here, which were obtained with  $12.0 \mu\text{J}/\text{cm}^2$  pump fluence and both pump and probe polarizations parallel to the NW axis. As the NW diameter decreases while approaching its tip, carriers relax much more rapidly. This tendency is explicitly shown by plotting the time constant,  $\tau$ , obtained from exponential curve fits to the measured  $\Delta T/T$  data, versus the NW diameter (Fig. 2(b)). This is consistent with previous measurements on NW ensembles, which demonstrated that surface-mediated mechanisms dominate their carrier dynamics, as their large surface-to-volume ratio makes them much more sensitive to these effects than the bulk material.<sup>8,9,12,28-31</sup>

Knowledge of the relaxation time constant also allows us to quantify transport properties, such as the carrier diffusion length. The diffusion length can be described by  $L_{\text{eff}} \propto \sqrt{D_{\text{eff}}\tau}$ ,<sup>12,32</sup> where  $L_{\text{eff}}$  is the effective diffusion length,  $D_{\text{eff}}$  is the diffusion constant, and  $\tau$  is the time constant described above. Our NWs are not expected to show any quantum confinement effects due to their relatively large diameter ( $d > 10$  nm); therefore, the parameters of undoped bulk Si can be used to interpret our results. Since we excite and observe both electron and hole dynamics in our experiments, we use  $D_{\text{eff}} = 24 \text{ cm}^2/\text{s}$ , defined here as an average diffusion constant of bulk Si for electrons and holes.<sup>33</sup> Fig. 2(b) clearly

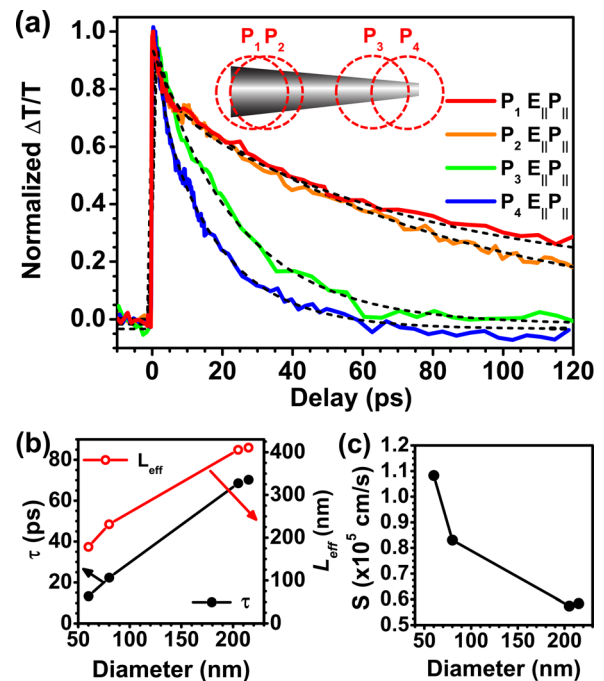


FIG. 2. (Color online) (a) Position-dependent transient transmission on a tapered single SiNW for both parallel polarizations. (b) Relaxation time,  $\tau$ , and diffusion length,  $L_{\text{eff}}$ , vs. diameter,  $d$ , for the tapered single SiNW. (c) Diameter dependence of the surface recombination velocity,  $S$ .

shows that  $L_{eff}$  increases with  $d$  (to  $L_{eff}=410.5$  nm on the large diameter ( $d=215$  nm) side of the NW). We find that the extracted diffusion lengths in our nanowires have somewhat larger values than those measured using different techniques.<sup>34</sup> This may be due to our use of a non-contact optical method for directly measuring the carrier lifetime, which eliminates contact-induced measurement effects. This is also influenced by the carrier concentration, since the measured lifetimes (and, therefore, the diffusion lengths) depend on carrier density (discussed in more detail below). Surface recombination velocities,  $S$ , can also be estimated from our results with a simple model<sup>32,34</sup> (Fig. 2(c)); we find the extracted values to compare reasonably well with others,<sup>27</sup> with a strong diameter dependence as observed in ZnO NWs.<sup>35</sup> The very low  $S$  values ( $<6 \times 10^4$  cm/s) obtained at large diameters ( $d > 150 \sim 200$  nm) are expected as surface states become less important in influencing recombination processes. This is also consistent with  $S \sim 3 \times 10^4$  cm/s for bulk Si, which has been shown elsewhere.<sup>27</sup>

The time-dependent photoinduced transmission change in single NWs can also be affected by the light polarization, as revealed through polarization-dependent experiments on single and ensemble NW samples. Figure 3(a) compares the

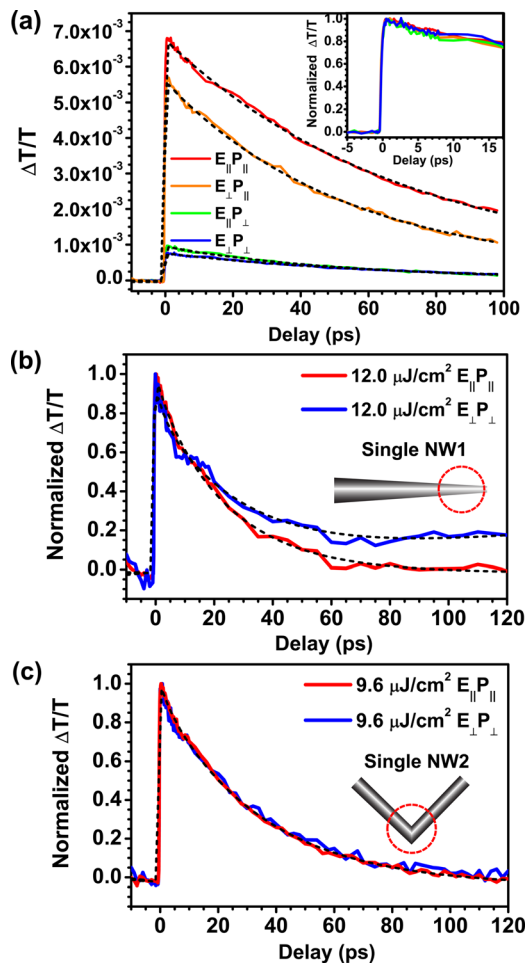


FIG. 3. (Color online) (a) Polarization-dependent ultrafast transmission measurements on ensemble SiNWs. The inset shows the normalized transient transmission for different pump and probe polarization combinations. The normalized transient transmission for  $E_{||}, P_{||}$  and  $E_{\perp}, P_{\perp}$  is shown (b) at the small end of the single straight SiNW and (c) at the middle of the single bent NW.

measured transmission changes in SiNW ensembles for four different pump and probe polarization combinations; here, we use  $E_{||}$  and  $E_{\perp}$  to indicate pump polarizations parallel and perpendicular to the NW axis, and  $P_{||}$  and  $P_{\perp}$  to indicate probe polarizations parallel and perpendicular to the NW axis, respectively. The initial  $\Delta T/T$  signal is maximum for  $E_{||}$  and  $P_{||}$  and minimum for  $E_{\perp}$  and  $P_{\perp}$ . This is expected since light absorption is maximum for light polarized parallel to the NW axis<sup>6,7</sup>; however, there was no significant anisotropy in the measured relaxation times (Fig. 3(a) inset), consistent with our previous experiments, which were conducted at much higher pump fluences with different pump and probe wavelengths.<sup>11</sup> Similarly, a measurement near the tip of the single SiNW reveals that the  $\Delta T/T$  signal is maximum for  $E_{||}$  and  $P_{||}$  and minimum for  $E_{\perp}$  and  $P_{\perp}$ . In stark contrast to the measurements on the NW ensemble, however, there is a clear anisotropy in the relaxation times measured for light polarized parallel and perpendicular to the long axis of the single SiNW, especially for smaller NW diameters (Fig. 3(b)). Overall, a faster decay was observed for  $E_{||}$  and  $P_{||}$  than  $E_{\perp}$  and  $P_{\perp}$ . This anisotropy in the measured dynamics decreases as the NW becomes larger and its properties become more bulk-like, which has also been observed in Ge NWs<sup>36</sup> and in core/shell GaAs/AlGaAs NWs.<sup>37</sup> This is due to decreases in the dielectric contrast between the NW and the surrounding material for optically thick NWs with a radius  $> \lambda/n_{nanowire}$  ( $d \sim 170$  nm in our case).<sup>13</sup> This can also help explain the absence of polarization dependent-dynamics in the NW ensemble: even in well aligned NW ensembles, the tapered shape of these NWs necessitates that there is a distribution of various diameters at any given point. The  $\Delta T/T$  signals will be dominated by the larger NWs, which may explain why we measured minimal polarization anisotropy in the carrier dynamics for ensembles, both here and in our previous experiments.<sup>11</sup>

In the single straight SiNW, more of the pump is absorbed for the parallel polarization, leading to a higher initial carrier density. Density-dependent effects such as Auger recombination, which typically cause decreasing carrier lifetimes with increasing carrier density,<sup>9,14,15</sup> may thus lead to the observed polarization dependence of the carrier dynamics. In contrast, a bent single NW with symmetric geometry has the same normalized  $\Delta T/T$  signal, irrespective of the light polarization (Fig. 3(c)), which demonstrates that the absorption is the same for both polarizations, resulting in minimal anisotropy in the measured dynamics.

To examine the influence of the photoexcited carrier density on polarization anisotropy in the single straight NW, we increased the pump fluence from  $1.4 \mu\text{J}/\text{cm}^2$  to  $12.0 \mu\text{J}/\text{cm}^2$  with  $E_{||}$  and  $P_{||}$  at the small end of the NW (Fig. 4(a)). Similar experiments were also performed with  $E_{\perp}$  and  $P_{\perp}$  (not shown). We then analyzed the effect of the carrier density on dynamic polarization anisotropy by estimating the linear absorption cross section of the NW for each polarization state from a generalized treatment of the linear absorption model in Ref. 13. Based on these expressions, we obtained the NW absorption cross sections to be  $\sigma_{||} = 8.99 \times 10^{-7} \text{cm}^2/\mu\text{m}$  for the parallel polarization and  $\sigma_{\perp} = 2.15 \times 10^{-7} \text{cm}^2/\mu\text{m}$  for the perpendicular polarization, respectively, at our 420 nm pump wavelength. The initial photoexcited carrier density in the NW,  $n(0)$ , can then be calculated using the expression



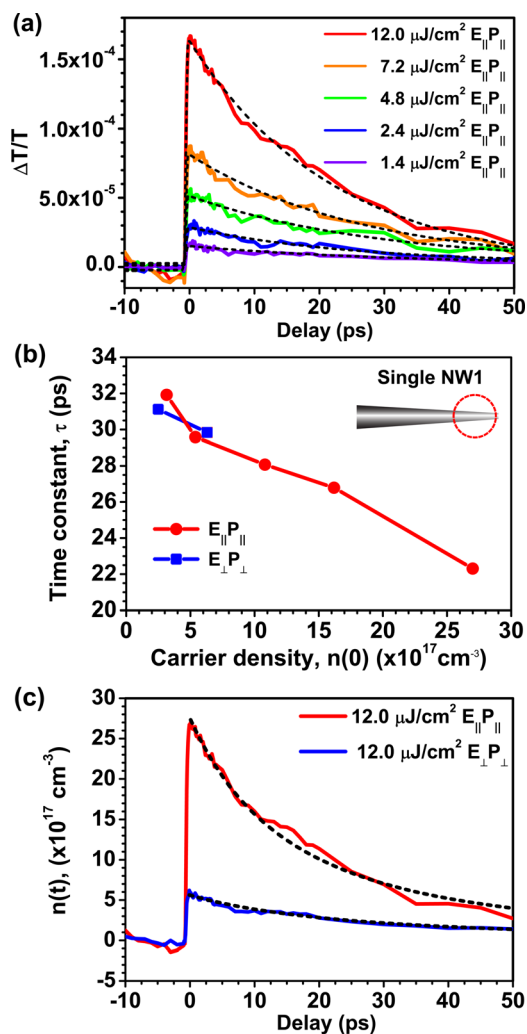


FIG. 4. (Color online) (a) Pump-fluence-dependent carrier dynamics at the small end of the straight NW for  $E_{\parallel}$  and  $P_{\parallel}$ . (b) Relaxation time constant vs. initial carrier density for two polarization configurations. (c) Fits to our data with an expression for three-carrier Auger recombination.

$n(0) = F\sigma/V$ , where  $F$  is the pump fluence,  $\sigma$  is the absorption cross section, and  $V$  is its volume.<sup>14</sup> Using this expression, the density-dependent relaxation time constants,  $\tau_{\parallel}$  and  $\tau_{\perp}$ , are plotted for two different polarizations (Fig. 4(b)), revealing that both time constants decrease with increasing carrier density. For  $n(0) \leq 7.0 \times 10^{17} \text{cm}^{-3}$ , the measured  $\tau_{\parallel}$  and  $\tau_{\perp}$  are comparable. This result supports the hypothesis that the polarization anisotropy in the measured dynamics is primarily governed by the density dependence of the carrier relaxation process. Similar polarization dependence was observed in carbon nanotube bundles using ultrafast pump-probe spectroscopy.<sup>38</sup>

To understand the physical mechanism underlying the density-dependent dynamics, we applied an Auger recombination model for 1D structures, in which the recombination process is generally governed by exciton-exciton bimolecular annihilation or a three-carrier (bulk-like) mechanism.<sup>14,39,40</sup> In our case, the three-carrier mechanism is likely to be the dominant process consistent with the measured decay kinetics, because quantum confinement effects are not expected, as discussed above. The time-dependent carrier density can be then described by<sup>14</sup>

$$n(t) = \frac{n(0)}{\left(1 + \frac{1}{D-1} C_D n(0)^{D-1} t\right)^{D-1}}, \quad (1)$$

where  $D=3$  for the three-carrier mechanism and  $C_3 = 1.5 \times 10^{-30} \text{cm}^6/\text{s}$  is a calculated third order Auger constant, representing the recombination probability in the NWs. The fits to our measured data using Eq. (1) were performed for two different polarization cases, indicating that the physical origin of the density dependence in our system is likely to be Auger recombination (Fig. 4(c)).

In conclusion, we have measured transient carrier dynamics in single Si nanowires, providing insight into light-matter interactions in quasi-1D nanosystems that is unattainable from ensemble studies. Through performing polarization- and spatially-resolved ultrafast optical spectroscopy, we demonstrated that carrier relaxation in single Si NWs is primarily governed by surface-mediated mechanisms and Auger recombination, with their relative importance depending on the NW size and morphology as well as the polarization and intensity of the incident light. Furthermore, our time-resolved optical experiments also enable us to accurately extract device-relevant parameters such as the diffusion length and surface recombination velocity in a non-contact manner, which can be directly compared to known values from electrical contact-based methods. These experiments thus reveal that by carefully controlling growth and experimental parameters, it should be possible to tailor carrier relaxation in a single Si nanowire for a given purpose. This could then enable better design of semiconductor NW-based devices for advanced applications, such as polarization-sensitive photodetection, high speed transistors, and solar energy harvesting at the nanoscale, where directional control and high spatial resolution are much desired. Finally, we also expect that future experiments on smaller nanowires, with diameters between 3-20 nm, will enable us to explore the influence of 1D quantum confinement on carrier dynamics, potentially uncovering a variety of unique phenomena.

Work at Los Alamos National Laboratory and Sandia National Laboratories was performed under the auspices of the U.S. Department of Energy, under Contract Nos. DE-AC52-06NA25396 and DE-AC04-94AL85000, respectively. This research was performed at the Center for Integrated Nanotechnologies (CINT), a U.S. Department of Energy (DOE), Office of Basic Energy Sciences (BES) user facility and supported in part by CINT and by the Laboratory Directed Research and Development Program. We also acknowledge the DOE BES, DMSE for supporting the development of ultrafast single nanowire spectroscopy.

<sup>1</sup>X. Duan, Y. Huang, R. Agarwal, and C. M. Lieber, *Nature* **421**, 241 (2003).

<sup>2</sup>C. Thelander, P. Agarwal, S. Brongersma, J. Eymery, L. F. Feiner, A. Forchel, M. Scheffler, W. Riess, B. J. Ohlsson, U. Gösele *et al.*, *Mater. Today* **9**, 28 (2006).

<sup>3</sup>P. J. Pauzauskie and P. Yang, *Mater. Today* **9**, 36 (2006).

<sup>4</sup>D. D. Ma, C. S. Lee, F. C. K. Au, S. Y. Tong, and S. T. Lee, *Science* **299**, 1874 (2003).

<sup>5</sup>T. V. Torchynska, M. M. Rodriguez, F. G. B. Espinoza, L. Yu Khomenkova, N. E. Korsunskaya, and L. V. Scherbina, *Phys. Rev. B* **65**, 115313 (2002).

<sup>6</sup>D. D. Ma, S. T. Lee, and J. Shinar, *Appl. Phys. Lett.* **87**, 033107 (2005).

- <sup>7</sup>J. Wang, M. S. Gudiksen, X. Duan, Y. Cui, and C. M. Lieber, *Science* **293**, 1455 (2001).
- <sup>8</sup>P. Parkinson, H. J. Joyce, Q. Gao, H. H. Tan, X. Zhang, J. Zou, C. Jagadish, L. M. Herz, and M. B. Johnston, *Nano Lett.* **9**, 3349 (2009).
- <sup>9</sup>R. P. Prasankumar, P. C. Upadhy, and A. J. Taylor, *Phys. Status Solidi B* **246**, 1973 (2009).
- <sup>10</sup>A. Othonos, E. Lioudakis, U. Philipose, and H. E. Ruda, *Appl. Phys. Lett.* **91**, 241113 (2007).
- <sup>11</sup>A. Kar, P. C. Upadhy, S. A. Dayeh, S. T. Picraux, A. J. Taylor, and R. P. Prasankumar, *IEEE J. Sel. Top. Quantum Electron.* **17**, 889 (2011).
- <sup>12</sup>R. P. Prasankumar, S. Choi, S. A. Trugman, S. T. Picraux, and A. J. Taylor, *Nano Lett.* **8**, 1619 (2008).
- <sup>13</sup>J. Giblin, V. Protasenko, and M. Kuno, *ACS Nano* **3**, 1979 (2009).
- <sup>14</sup>I. Robel, B. A. Bunker, P. V. Kamat, and M. Kuno, *Nano Lett.* **6**, 1344 (2006).
- <sup>15</sup>H. Htoon, J. A. Hollingsworth, R. Dickerson, and V. I. Klimov, *Phys. Rev. Lett.* **91**, 227401 (2003).
- <sup>16</sup>G. V. Hartland, *Chem. Sci.* **1**, 303 (2010).
- <sup>17</sup>C. R. Carey, Y. Yu, M. Kuno, and G. V. Hartland, *J. Phys. Chem. C* **113**, 19077 (2009).
- <sup>18</sup>J. C. Johnson, H.-J. Choi, K. P. Knutsen, R. D. Schaller, P. Yang, and R. J. Saykally, *Nature Mater.* **1**, 106 (2002).
- <sup>19</sup>S. Chu, G. Wang, W. Zhou, Y. Lin, L. Chernyak, J. Zhao, J. Kong, L. Li, J. Ren, and J. Liu, *Nat. Nanotechnol.* **6**, 506 (2011).
- <sup>20</sup>E. C. Garnett and P. Yang, *J. Am. Chem. Soc.* **130**, 9224 (2008).
- <sup>21</sup>L. Tsakalacos, *Appl. Phys. Lett.* **91**, 233117 (2007).
- <sup>22</sup>B. M. Kayes, H. A. Atwater, and N. S. Lewis, *J. Appl. Phys.* **97**, 114302 (2005).
- <sup>23</sup>B. Tian, X. Zheng, T. J. Kempa, Y. Fang, N. Yu, G. Yu, J. Huang, and C. M. Lieber, *Nature* **449**, 885 (2007).
- <sup>24</sup>S. Hoffmann, J. Bauer, C. Ronning, T. Stelzner, J. Michler, C. Ballif, V. Sivakov, and S. H. Christiansen, *Nano Lett.* **9**, 1341 (2009).
- <sup>25</sup>M. D. Kelzenberg, D. B. Turner-Evans, B. M. Kayes, M. A. Filler, M. C. Putnam, N. S. Lewis, and H. A. Atwater, *Nano Lett.* **8**, 710 (2008).
- <sup>26</sup>S. T. Picraux, S. A. Dayeh, P. Manandhar, D. E. Perea, and S. Choi, *JOM* **62**, 35 (2010).
- <sup>27</sup>A. J. Sabbah and D. M. Riffe, *Phys. Rev. B* **66**, 165217 (2002).
- <sup>28</sup>T. Hanrath and B. A. Korgel, *J. Phys. Chem. B* **109**, 5518 (2005).
- <sup>29</sup>S. A. Dayeh, C. Soci, P. K. L. Yu, E. T. Yu, and D. Wang, *Appl. Phys. Lett.* **90**, 162112 (2007).
- <sup>30</sup>R. Calarco, M. Marso, T. Richter, A. I. Aykanat, R. Meijers, A. v.d. Hart, T. Stoica, and H. Lüth, *Nano Lett.* **5**, 981 (2005).
- <sup>31</sup>S. A. Dayeh, E. T. Yu, and D. Wang, *Small* **5**, 77 (2009).
- <sup>32</sup>J. E. Allen, E. R. Hemesath, D. E. Perea, J. L. Lensch-Falk, Z. Y. Li, F. Yin, M. H. Gass, P. Wang, A. L. Bleloch, R. E. Palmer *et al.*, *Nat. Nanotechnol.* **3**, 168 (2008).
- <sup>33</sup>D. F. Edwards, *Handbook of Optical Constants of Solids* (Academic, Orlando, Fla., 1985).
- <sup>34</sup>Y. Dan, K. Seo, K. Takei, J. H. Meza, A. Javey, and K. B. Crozier, *Nano Lett.* **11**, 2527 (2011).
- <sup>35</sup>A. Soudi, P. Dhakal, and Y. Gu, *Appl. Phys. Lett.* **96**, 253115 (2010).
- <sup>36</sup>L. Cao, J. S. White, J.-S. Park, J. A. Schuller, B. M. Clemens, and M. L. Brongersma, *Nature Mater.* **8**, 643 (2009).
- <sup>37</sup>A. Persano, B. Nabet, A. Taurino, P. Prete, N. Lovergine, and A. Cola, *Appl. Phys. Lett.* **98**, 153106 (2011).
- <sup>38</sup>Y. Hashimoto, Y. Murakami, S. Maruyama, and J. Kono, *Phys. Rev. B* **75**, 245408 (2007).
- <sup>39</sup>V. I. Klimov, *J. Phys. Chem. B* **104**, 6112 (2000).
- <sup>40</sup>T. Bittner, K.-D. Irrgang, G. Renger, and M. R. Wasielewski, *J. Phys. Chem.* **98**, 11821 (1994).